Structural Safety Evaluation for the Driving part of 15kW-Class HATCT Model by FSI Analysis

Ming Guo[#1], Seung-Jun Kim[#1], Young-Do Choi [*2]

[#]*Graduate School, Department of Mechanical Engineering, Mokpo National University, 1666 Youngsan-Ro, Cheonggye-Myeon, Muan-gun, Jeonnam, 58554, Republic of Korea*

[1]guominglab@163.com

[*]*Department of Mechanical Engineering, Mokpo National University, 1666 Youngsan-Ro, Cheonggye-Myeon, Muan-gun, Jeonnam, 58554, Republic* of Korea

[2]ydchoi@mokpo.ac.kr

***Abstract*— For the design of tidal current turbine, there are hydrodynamic design and structural design, which should be considered. The design methods must be satisfied with the performance and structural safety for its feasibility. Most of the tidal current turbine requires hydrodynamic design in order to improve the efficiency and performance. It is necessary to have a clear understanding of the characteristics of the blade adjacent flow field. The casing and shaft of tidal current turbine driving part, which is affected from flow field, needs to be designed and evaluated for structure safety to withstand all the harsh conditions of the sea. In this study, driving part of tidal current turbine was investigated by evaluating structural safety with analysis of one way fluid structure interaction (FSI) analysis. The fluid structure interaction analysis of driving part was conducted for different shapes of driving part with same 15kW-class tidal current turbine blade. For conducting reliable evaluation of structural safety, the surface load(pressure) of the tidal current turbine driving part is obtained from CFD analysis for initial condition of FSI analysis.**

***Keywords*— Tidal current turbine, Driving part, Fluid Structure Interaction (FSI), Design method, Computational Fluid Dynamic (CFD)**

I. INTRODUCTION

The tidal current turbine (TCT) is an effective device, used for the tidal current energy conversion. The blade is the core component of a tidal current turbine which determines whether the apparatus can achieve a good efficiency or not. In addition, more attention should also be paid to the structural safety evaluation. The design of tidal current turbine consists of hydrodynamic design and structural design. During the design process, the reliability of The tidal current turbine (TCT) need to be higher to stand the harsh marine environment. [1, 2]

In this study, the hydrodynamic design of the 15kW turbine blade and the structural design of the driving part were carried out respectively, and the structural safety evaluation of the driving part was evaluated by applying the unidirectional fluid structure interaction analysis. Moreover, the same rotor blade of 15kW-class tidal current turbine assembled with different driving parts were conducted, the surface pressure distribution obtained from CFD analysis was used as the initial condition for unidirectional fluid – structure analysis. Therefore, The evaluation of reliable structural safety could be obtained.[4,5,6,8]

II. TIDAL CURRENT TURBINE MODEL

A. Design of Tidal Current Turbine

Table I shows the basic design parameters of the tidal current turbine model blade, and Blade element momentum theory [7] was adopted in the design process. Fig. 1 shows the distribution of string length and twist angle according to the blade design method. MNU26 hydrofoil [8], used for different cross sections, was developed properly from the blade tip to the hub, and it was developed by a kind of air foil. Fig. 2 shows the three dimensional modelling of the tidal current turbine chord length and twist angle.

TABLE I
DESIGN PARAMETERS FOR BLADE DESIGN

Design Parameters	Values
P_{rated}: Rated power	15 kW
V_{rated}: Rated current velocity	2
ρ: Sea water density	1024 kg/m^3
λ: Tip speed ratio	5
D: Rotor diameter	3.5 m
N: Number of blade	3
ω: Rotational speed	54.56 min^{-1}

B. The Driving Part of Tidal Current Turbine Model

In this study, the previous study of 50W-class current turbine model was taken as the reference for the design of casing and shaft of the 15kW-class driving part. In order to investigate the structural safety of the driving part for the flow around the turbine, different types of driving parts have been designed, and Fig. 3 shows the driving parts of Type 1 and Type 3. For the shape of the driving part, Type 3 was selected as the fluid - structure analysis model. Moreover, five driving parts were designed based on the Type 3, and the five

configuration of different driving parts were illustrated in table II.

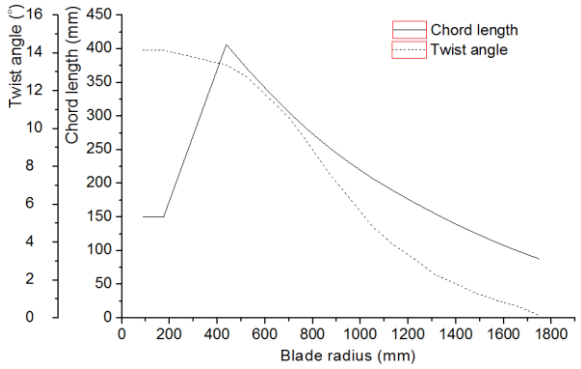

Fig. 1 Twist angle and chord length according to blade radius of the 15kW-class tidal current turbine blade

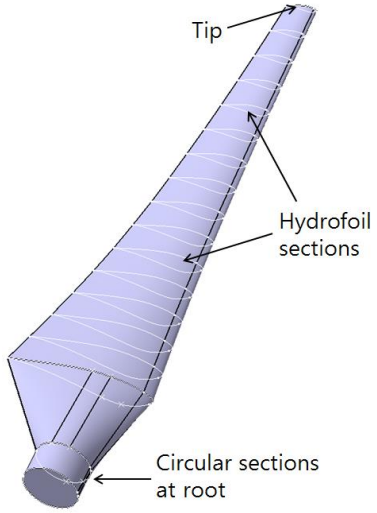

Fig. 2 3D model of tidal current turbine blade

TABLE II
DIFFERENT CASES OF DRIVING PART

Condition	Driving part	
	Length(L1)	Length(L2)
Type 1	1	4
Type 2	1	2
Type 3	1	1
Type 4	2	2
Type 5	2	1

III. NUMERICAL METHOD

A. *Numerical Grid and Boundary Conditions*

Fig. 4 shows the numerical grid of full domain for 15kW-class tidal current turbine.

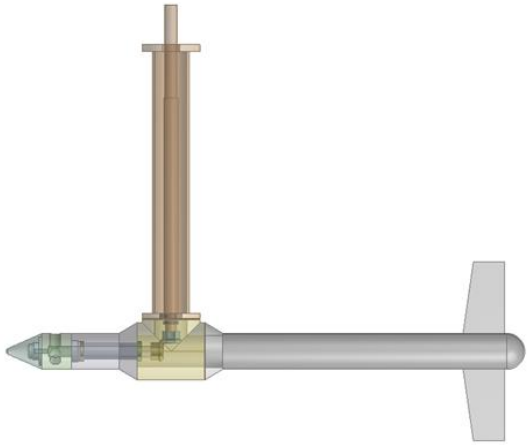

(a) Analysis model of Type 1

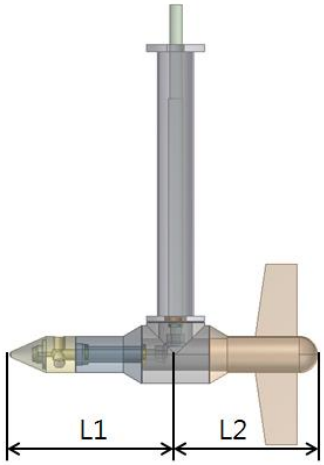

(b) Analysis model of Type 3

Fig. 3 Different driving part of tidal current turbine model for FSI analysis

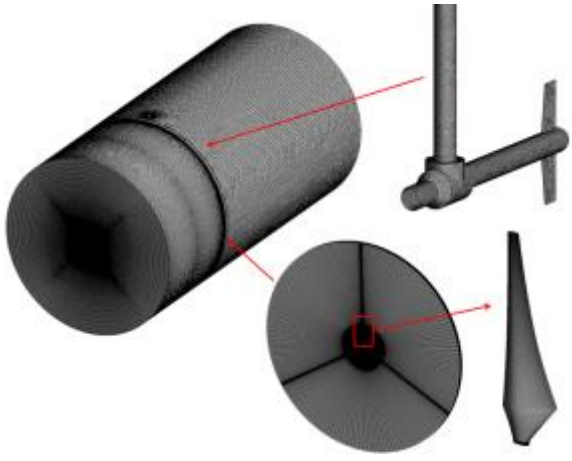

Fig. 4 Numerical grid of the 15kW- class tidal current turbine model

The inlet and outlet lengths were set by 3 and 7 times of the blade radius, respectively. The radial distance was set by 3

times of the blade radius. The inlet and outlet domains were constructed with hexahedral structural grids, and total element number is 14.6×10^6 and total nodes number is 14.3×10^6. The outlet parts, connected to the driving parts, were constructed with tetrahedral structural grids and there are slightly different number of elements and nodes depending on the shape of the driving part.

For numerical analysis of tidal current turbine model, ANSYS CFX[9] was used as a solver in this study. Table III presents the boundary conditions of the computational flow fields for the numerical analysis of the tidal current turbine model. The same boundary conditions have been applied in different types of the driving parts.

TABLE III
BOUNDARY CONDITIONS FOR ANALYSIS

Condition	Values
Inlet	Stream velocity
Outlet	Static pressure
Interface	Frozen rotor
Calculation type	Steady state
Wall	No-slip
Working fluid	Sea water at 25 ℃
Tidal current speed	2 m/s
Turbulence model	SST

B. *Result of CFD Analysis*

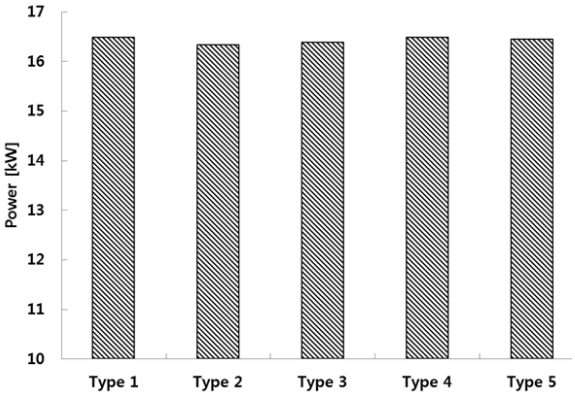

Fig. 5. Output Power produced by 15kW-class tidal current turbine model of different driving parts

Fig. 5 shows the output power produced by 15kW-class tidal current turbine model with different driving parts. The rotor blade with different driving parts showed a similar output power from the lowest 16.3kW to the highest 16.4kW. Therefore, it can be confirmed that the designed rotor blades have reached the target output power of 15 kW and the desirable design has been achieved. Fig. 6 and Fig. 7 show the pressure contour distribution and stream line distribution on the driving part of 15kW-class tidal current turbine model. Different types of driving parts also indicate similar pressure contour distribution and streamline distribution. In the streamline distribution of the tidal current turbine model, many streamlines are visible behind the driving part, In the pressure distribution, a relatively high pressure is observed on the surface of the vertical axis casing which is connected to the driving part. Among the results of CFD analysis performed on the different types of driving part, the surface load (static pressure) of the driving part casing was set as the initial load condition of the three dimensional model for unidirectional fluid structure interaction analysis.

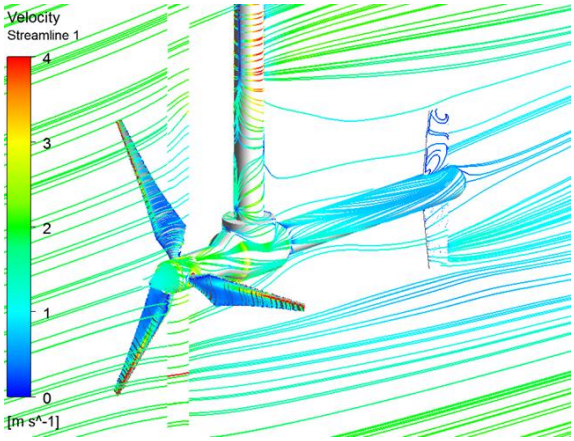

Fig. 6 Streamline distribution of 15kW-class tidal current turbine model

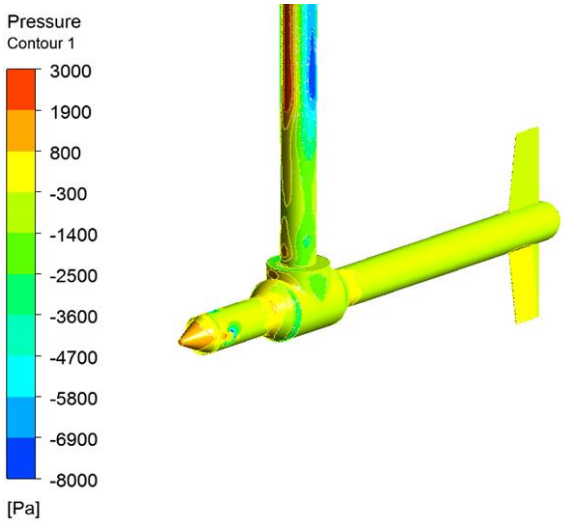

Fig. 7 Static pressure contour of 15kW-class tidal current turbine model

IV. FLUID STRUCTURE INTERACTION(FSI) ANALYSIS

A. *Numerical Grid And Boundary Conditions of FSI Analysis*

The analysis of one way fluid structure interaction was conducted by ANSYS CFX. Fig. 8 shows the numerical grid of driving part for FSI analysis. Tetrahedral mesh was applied. Table IV presents the numerical grid element number and node number for each case with different driving parts.

Fig. 9 and Table V show the boundary conditions for one way fluid structure interaction analysis. From the results of the flow analysis, the surface load (static pressure) value of the

tidal current turbine was set as the initial load condition, and the rotational speed of the rotor blade was applied in the hub. Fixed support was set on the upper surface of the central axis casing in the vertical direction of the driving part. The gravity condition was also set in the turbine driving part. Table VI shows material propriety of stainless steel, which was used for FSI analysis.

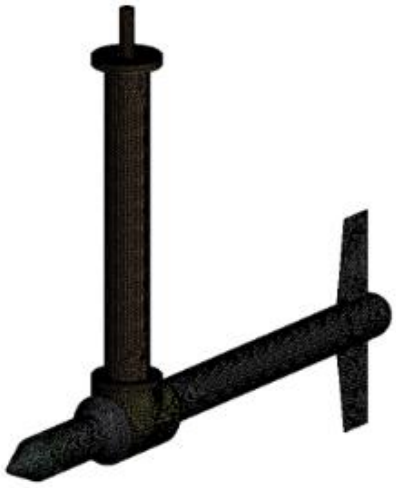

Fig. 8 Numerical grid of driving part for FSI analysis

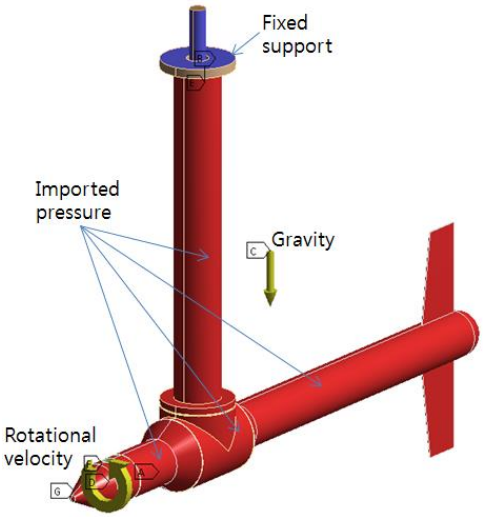

Fig. 9 Boundary conditions for FSI analysis

TABLE IV
NUMERICAL GRID FOR DIFFERENT TYPES OF DRIVING PART

Condition	Element No.	Nodes No.
Type 1	4.5×10^5	7.2×10^5
Type 2	4.3×10^5	6.8×10^5
Type 3	4.1×10^5	6.5×10^5
Type 4	4.9×10^5	7.7×10^5
Type 5	4.8×10^5	7.5×10^5

TABLE V
BOUNDARY CONDITIONS FOR FSI ANALYSIS

Condition	Values
Supports	Fixed support
Gravity	9.807 m/s^2
Rotational speed	5.714 rad/s
Imported solution	CFX-Fluid Flow
Imported load	Pressure

TABLE VI
MATERIAL PROPERTY FOR STAINLESS STEEL

Property	Stainless Steel
Density (kg/m3)	7750
Young's modulus (MPa)	1.93×10^5
Poisson's ratio	0.31
Tensile yield strength (MPa)	207
Compressive yield strength (MPa)	207

B. *Result and Discussion*

One way FSI analysis of the turbine driving part was performed to evaluate the structural safety of the casing and shaft. The maximum equivalent stress and deformation of the driving part can be obtained. The results of FSI analysis of the different types of driving part were compared.

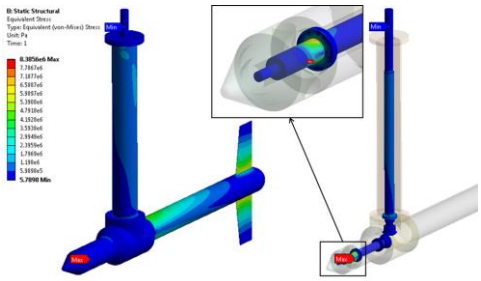

(a) Analysis model of Type 1

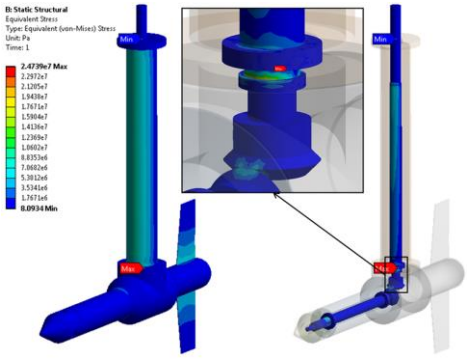

(b) Analysis model of Type 5

Fig. 10 Equivalent stress distribution of driving part

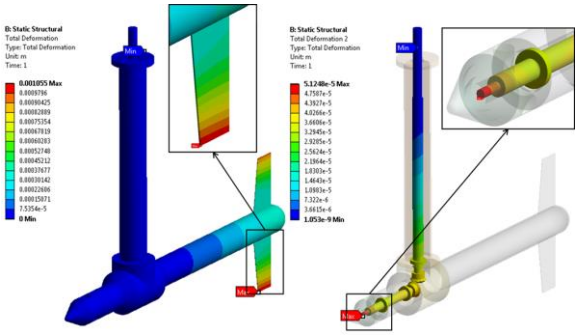

(a) Analysis model of Type 1

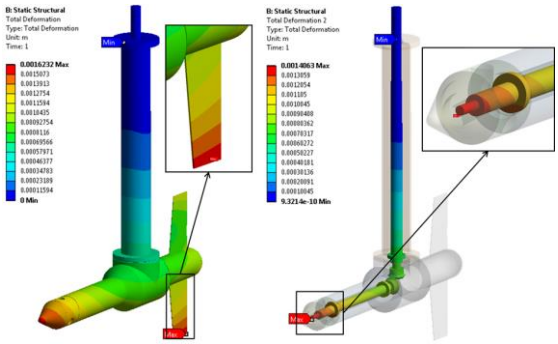

(b) Analysis model of Type 5

Fig. 11 Total deformation of driving part

Fig. 10 shows the maximum equivalent stresses of Type 1 and Type 5, respectively. The position of the maximum equivalent stress value was obtained at a similar location for Type 1, 2, 3. A similar trend was observed for Type 4 and 5. Additionally, it was confirmed that the maximum equivalent stress occurrence position of the blade differs regarding the length of the casing. The shape of all the driving parts, for which the FSI analysis was performed, showed higher equivalent stress on the inner shaft than outer casing. The casing of the driving part shows a relatively low equivalent stress in the whole, whereas the rudder part shows the relatively high equivalent stress.

Fig. 11 shows the total deformation of Type 1 and Type 5, the outer casing and inner shaft of driving part showed different values of total deformation. The maximum deformation was shown at the rudder part of outer casing and tip of blade shaft in inner shaft. The maximum deformation of the rudder can be judged by the flow characteristics of the tidal current turbine rotor blade.

The maximum equivalent stresses of the different types of driving parts are compared with the tensile yield strength of stainless steel as shown in Fig. 12. The minimum equivalent stress was observed in Type 1. The maximum value in Type 5 is about 3 times as larger as the minimum equivalent stress of Type 1. However, the equivalent stress value of Type 5 has very low value compared with the tensile yield strength of stainless steel. Therefore, structural safety can be confirmed.

Fig. 13 shows the maximum deformation of the driving part, and it is compared with the casing and shaft. The maximum deformations shown in the casing occurred at the rudder end. The maximum deformation of shaft occurred from the tip in the blade hub direction. A similar trend is observed with a shorter distance between the rudder and the center shaft casing. Type 5 showed the maximum deformation of 0.0016 m among all the cases. It can be confirmed that the structure of this turbine is safe.

.

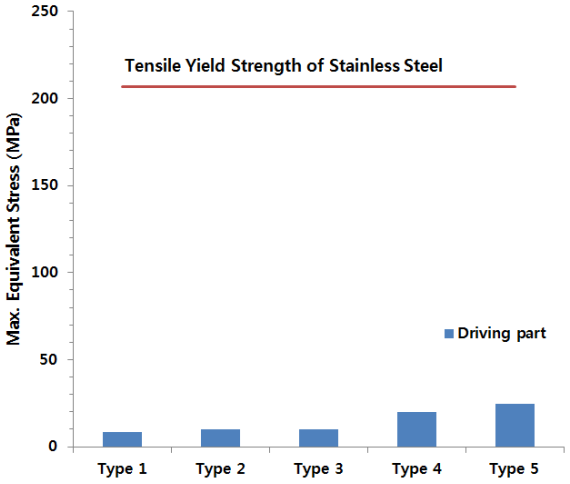

Fig. 12 Comparison of maximum stresses on all cases

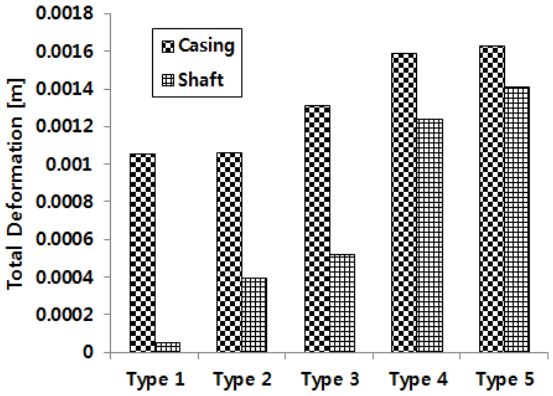

Fig. 13 Comparison of maximum deformation on all cases

V. Conclusions

In this study, the hydrodynamic design of the 15kW-class turbine blade model and the structural design of the driving part have been carried out, respectively. The result from the FSI analysis for the design condition concluded that the rotor blade is structurally safe for application. The maximum equivalent stress is found around hub of rotor blade and maximum deformation is found at the trailing edge of rotor blade tip in all rotor blades.

REFERENCES

[1] B.-S. Kim, K.-S. Lee, and M.-E. Kim, "Design of a 2MW Blade for Wind Turbine and Uni-Directional Fluid Structure Interaction Simulation," *Transactions of the Korean Society of Mechanical Engineers B*, 2009. vol. 33, no. 12, pp. 1007-1013,

[2] P. M. Singh, Z. M. Chen, and Y.-D. Choi, "Numerical analysis for a proposed hybrid system with single HAWT, double HATCT and vertical oscillating wave energy converters on a single tower," *Journal of Mechanical Science and Technology*, 2016. vol. 30 no. 10, pp. 1-11,

[3] Y.-G. Kim, and K.-C. Kim, "Analysis of Fluid Structure Interaction on 100kW-HAWT-blade," *Journal of the Korean Society of Visualization*, 2006. vol. 4, no. 1, pp. 41-46,

[4] P. M. Singh, Z. M. Chen, and Y.-D. Choi, "15kW-class wave energy converter floater design and structural analysis," *Journal of the Korean Society of Marine Engineering*, 2016. vol. 40, no. 2, pp. 146-151,

[5] Z. M. Chen, P. M. Singh, and Y.-D. Choi, "Structural Analysis on the Arm and Floater Structure of a Wave Energy Converter," *Journal of Fluid Machinery*, 2015. vol. 18, no. 3, pp. 5-11,

[6] C.-H. Jo, D.-Y. Kim, Y.-H. Rho, K.-H. Lee, and C. Johnstone, "FSI analysis of deformation along offshore pile structure for tidal current power," *Renewable energy*, 2013. vol. 54, pp. 248-252,

[7] T. Burton, D. Sharpe, N. Jenkins, and E. Bossanyi, *Wind Energy Handbook*, John Wiley & Sons, Ltd., 2001.

[8] P. M. Singh, and Y.-D. Choi, "Shape design and numerical analysis on a 1MW tidal current turbine for the south-western coast of Korea," *Renewable Energy*, vol. 68, pp. 485-493, 2014.

[9] ANSYS Inc, "ANSYS CFX Documentation," Ver. 18.1 http://www.ansys.com, 2017.